E116

The Source of 1960 Chile Earthquake from What We Have Learned in The 2011 Tohoku Tsunami

〇Tung-Cheng HO, Kenji SATAKE, Shingo WATADA, Yushiro FUJII

The Tsunami Speed Reduction

Systemic travel time delays of up to 15 min relative to the linear long waves for transoceanic tsunamis have been reported. A phase correction method, which converts the linear long waves into dispersive waves, was previously proposed to consider seawater compressibility, the elasticity of the Earth, gravitational potential change associated with tsunami motion, ocean density stratification, actual raypath, and actual bathymetry.

Those factors explained the travel time delay of up to 1.5% on average at the far-field stations. The 1.5% travel time delay is neglectable in near field. However, the 1.5% delay is equal to 18 min when a tsunami traveled 20 hours. For transoceanic tsunamis, the factors are necessary to perform accurate tsunami predictions. Moreover, the improved phase correction method provides an efficient way to correct linear long waves, which is suitable for existing tsunami forecasting and source inversions.

The 1960 Chile earthquake

The 1960 Chile earthquake occurred in southern Chile on 22 May 1960 is known as the largest instrumentally recorded earthquake. Because of the data saturation and insufficient observation, the estimated magnitude of this earthquake ranges from M 9.2 to M 9.6 among studies using different types of data, including seismic data, geodetic data, and tsunami data. The 1960 earthquake caused severe damage and significant ground movement in southern Chile.

The Ground Deformation

Plafker and Savage (1970) measured and reported the coastal vertical change and leveling data at the source region. The coastal elevation change data were measured in 1968 at 155 locations from about 36°S to 46°S. The largest uplift was recorded in the Guamblin Island with about 5.7 m, and the largest subsidence was -2.7 m recorded in Valdivia city.

The leveling data are the vertical displacements along the Inter-American Highway of postearthquake (1963–1964) relative to preearthquake (1957–1959).

The coastal vertical change and leveling data are used to estimate the slip distribution by Barrientos and Ward (1990), Moreno et al. (2009) Fujii and Satake (2013), and this study.

The Tsunami after the 1960 Earthquake

The ground deformation also took place on the seafloor and triggered a large tsunami. The tsunami waves were observed by dozens of tide gauges in Chile, Peru, Ecuador, Colombia, Mexico, the United States, Canada, Australia, the Philippines, Taiwan, Japan, Hawaii, and many islands in the Pacific Ocean (Berkman & Symons, 1964).

At near field (traveltime < 3 hr), this tsunami caused 3-m-high waves in Talcahuano (Chile). For far-field, the largest wave was recorded in Hakodate (Japan) with up to 2 m. Tide gauges on the West Coast of the United States and Hawaii also recorded large waves of about 1 m high.

Fujii and Satake (2013) digitized the tide gauge records compiled in Berkman and Symons (1964), and we resampled the waveform data with a 15-s interval.

In the present study, five near-field tsunami waveforms in Chile and 44 far-field waveforms were used to estimate the tsunami source (Figure 1).

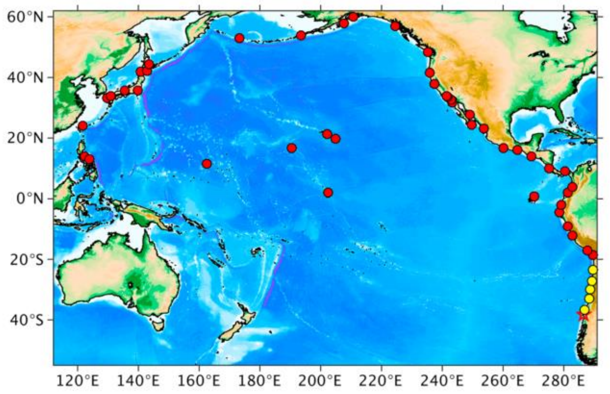

Figure 1. The computation domain and in this study. The yellow and red dots show the near-field and far-field tsunami stations. The red star represents the earthquake epicenter.

Joint Inversion Method

We applied the phase correction method to tsunami Green’s functions to incorporate the effects that explain the tsunami speed resuction. First, a joint inversion using tsunami waveforms and geodetic data was performed to estimate the tsunami source of sea surface elevation.

Finally, we estimate the slip distribution with the inverted sea surface elevation. We created 436 subfaults on the fault plane, which is based on the Slab 1.0 (Hayes et al., 2012) and depth data from Tassara and Echaurren (2012) for the deep region. We computed the sea surface elevation by applying the elastic half-space model (Okada, 1985), and then we utilized non-negative least-square method to estimate the slip distribution that fits the inverted tsunami source.

Results

Three asperities at the north 38°S to 41°S, central 41°S to 44°S, and south 44°S to 46°S were estimated in this study. The joint inversion shows that the central and south asperities contributed not only to the large coastal elevation changes in the southern source area but also to the tsunami waveforms at far field.

The magnitude of Mw 9.3 and 9.4 were estimated with assumed rake angles 90 and 140°, respectively. It is slightly larger than the estimations of Barrientos and Ward (1990), Moreno et al. (2009), and Fujii and Satake (2013) but smaller than those from seismic data (Kanamori & Anderson, 1975).

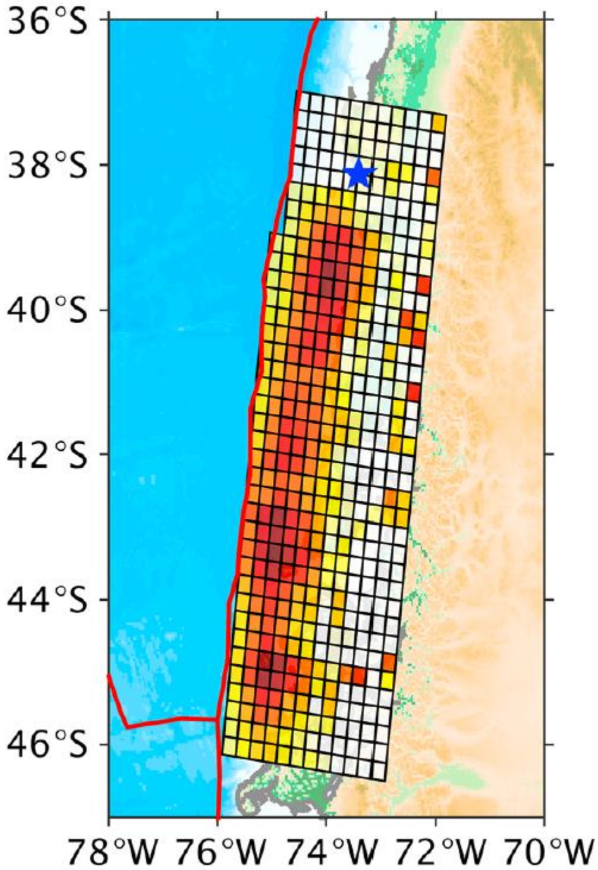

Figure 2. The estimated slip distribution in this study.

Discussion and Conclusion

The north asperity caused the major tsunami impact in the East Pacific coasts. The central and south asperities contributed to the tsunami waves in the islands in the Pacific Ocean. The three asperities arrived at the West Pacific coasts at the same time and caused destructive tsunamis in this region. The addition of far-field tsunami data provided us supplementary source information from different azimuthal directions that helped us to better understand the slip distribution of the megathrus.